Available online at www.sciencedirect.com
SCIENCE DIRECT®
International Journal of Pharmaceutics 297 (2005) 9–21
international journal of pharmaceutics
www.elsevier.com/locate/ijpharm

Model analysis of flux enhancement across hairless mouse skin induced by chemical permeation enhancers

Ning He, Kevin S. Warner, William I. Higuchi, S. Kevin Li *

Department of Pharmaceutics and Pharmaceutical Chemistry, College of Pharmacy, University of Utah, 30 S 2000 E, Rm 213, Salt Lake City, UT 84112, USA

Received 2 April 2004; received in revised form 21 September 2004; accepted 13 January 2005
Available online 20 April 2005

Abstract

Previous permeant partitioning studies with hairless mouse skin (HMS) in the presence of several chemical skin permeation enhancers have revealed that, when such enhancers induce significant skin permeability coefficient enhancement, it is accompanied by significant enhancement in the equilibrium uptake (partitioning) of the permeant into the intercellular lipid component of the stratum corneum (SC). Particularly, it was found that the 1-alkyl-2-pyrrolidones and the 1-alkyl-2-azacycloheptanones, at aqueous solution concentrations that gave skin permeation enhancement (E) of 10 for corticosterone (CS, the permeant), enhanced the equilibrium uptake of β-estradiol (E2β, a surrogate permeant) from the aqueous phase into the intercellular lipids of HMS SC by a factor of 5–7. This finding raised the question of whether this uptake enhancement induced by the permeation enhancer under equilibrium conditions would be essentially the same as that determined kinetically from time-dependent permeation experiments utilizing appropriate SC membrane models and Fick's laws of diffusion to treat the data. HMS transport experiments were conducted with CS as the permeant and 1-octyl-2-pyrrolidone (OP) and 1-hexyl-2-azacycloheptanone (HAZ) as the enhancers. In treating the experimental data, a one-layer skin transport model (SC only) and a two-layer model (SC layer and the epidermis/dermis layer) were both investigated. Both the partition coefficient enhancement (E_K) and the diffusion coefficient enhancement (E_D) were deduced from the data treatment. The results showed that when the total transport enhancement of CS was around 11, E_K was in the range of 6–8 and E_D was in the range of 1.5–1.9 using both the one-layer and the two-layer models. This E_K value was found to be in good agreement with the E2β partition enhancement obtained directly under equilibrium conditions in previous studies. This indicates that (a) the rate-limiting domain for the transport of the lipophilic permeants across HMS and the HMS SC intercellular lipid domain probed in the equilibrium partitioning experiments are essentially the same, and (b) the total flux enhancement (E) of lipophilic permeants across HMS was driven mainly by enhancing the partitioning of the permeant into the rate-limiting domain (E_K) and secondarily by enhancing the diffusion coefficients (E_D) of the permeant in the domain. Comparison of the one-layer and two-layer skin model results revealed that non-steady-state transport of lipophilic compounds across HMS was better described by the two-layer model because the dermis/viable epidermis played a significant role in lipophilic permeant binding.

Keywords: Chemical permeation enhancers; Enhancer mechanism; Transport model; Hairless mouse skin

* Corresponding author. Tel.: +1 801 581 4110; fax: +1 801 585 1270.
E-mail address: kevin.li@m.cc.utah.edu (S.K. Li).

0378-5173/$ – see front matter © 2005 Elsevier B.V. All rights reserved.
doi:10.1016/j.ijpharm.2005.01.041

1. Introduction

As part of the effort to better understand the mechanism of drug permeation across skin, many researchers have attempted to elucidate the action of chemical permeation enhancers in terms of increased permeant diffusion (D) and partition (K) coefficients. Some studies have been based on the assumption that full-thickness skin is a homogeneous membrane in order to simplify the analysis (Foreman and Kelly, 1976; Hashida et al., 1988; Okamoto et al., 1988). However, it should be more rigorous to consider skin as a two-layer membrane, because skin may be considered as of two main distinctive layers from the standpoint of transport—the stratum corneum (SC) and dermis/viable epidermis (D/E) (Tojo et al., 1987; Okamoto et al., 1989; Yamashita et al., 1993, 1994, 1995). Other studies have used SC instead of full-thickness skin in permeation and drug release experiments to study the barrier properties of SC (Mitragotri, 2000), in which case, the transport parameters K and D were estimated for the SC directly from the analyses of drug penetration and/or release profiles with mathematical models based upon Fick's laws of diffusion.

In previous studies conducted in our laboratory, the enhancement of the equilibrium partitioning of the lipophilic permeant, E2β, into the lipid domains of HMS SC was measured (Yoneto et al., 1998; He et al., 2003, 2004; Chantasart et al., 2004) in the presence of chemical permeation enhancers. It was found that the partitioning enhancement of E2β was in the range of 5–7 for the studied chemical permeation enhancers under isoenhancement conditions of $E = 10$ (aqueous concentrations for which the enhancers induced a 10-fold permeant transport enhancement for the lipoidal pathway of SC). An important question raised in these studies was: would the equilibrium partitioning enhancement data of E2β correspond to the partitioning enhancement of E2β for permeation across the SC determined in transport kinetics experiments? As part of our study of the mechanism of action of permeation enhancers, it was considered necessary to address this question. Comparable enhancer effects obtained from equilibrium partitioning experiments and from kinetic transport experiments would suggest that the intercellular lipid domain probed in the equilibrium partitioning experiments is the same as the transport rate-limiting domain for permeation across HMS SC.

The objective of the present study was to determine the enhancement of K and of D from transport kinetics of a model permeant across HMS in the presence of the chemical permeation enhancers under the isoenhancement conditions of $E = 10$ (Yoneto et al., 1998; He et al., 2003, 2004; Chantasart et al., 2004). These coefficients were to be determined by analyzing permeation data (both non-steady-state and steady-state) with theoretical transport models (one-layer and two-layer skin models). The enhancer effects upon the partitioning of the permeant into the rate-limiting domain for permeation across HMS would then be examined and compared to those for permeant uptake into the HMS SC lipids obtained in the previous equilibrium partitioning studies.

2. Experimental

2.1. Strategy

A direct comparison of the partitioning enhancement data obtained from kinetic transport experiments and those from the equilibrium partitioning experiments of E2β was not practical due to the D/E layer being a significant barrier for E2β permeation across HMS. Moreover, significant E2β metabolism was observed in E2β transdermal penetration (over 60% of ^{3}H-E2β converted to metabolites in the receiver chamber at the end of HMS transport experiments; Liu, 1989). Because of these difficulties, non-steady-state E2β transport analysis was considered to be too complicated, and CS was considered as the surrogate permeant for E2β in the present study. On the other hand, CS was considered not to be an appropriate probe molecule in the equilibrium partitioning experiments because of the relative large amount of CS uptake into the non-lipid domain of SC (due to the relatively low lipophilicity of CS compared with E2β). Preliminary equilibrium partitioning experiments showed that the uptake of CS into the intercellular lipid domain of HMS SC could not be determined accurately. Because of this, it was decided to employ a strategy based upon examining the relationship between the kinetically deduced transport partitioning enhancement of CS and the equilibrium partitioning enhancement of E2β. This strategy was considered appropriate because previous studies had shown similar transport enhancement

effects of chemical enhancers upon E2β and CS permeation across the lipoidal pathway of HMS SC (Yoneto et al., 1995). In the present study, transport experiments were to be first conducted with both E2β and CS under the same experimental conditions, and the transport enhancement of E2β and CS across the lipoidal pathway of SC were to be determined. Once the relationship between the transport enhancement of E2β and CS was established and verified, HMS transport experiments were to be conducted with CS to determine the *K* and *D* enhancement factors using a theoretical one-layer skin transport model. A theoretical two-layer skin transport model was also examined. In the two-layer model study, the D/E layer of HMS was to be first characterized in partition and permeation experiments with stripped HMS using CS and a water marker, raffinose. Then, the enhancement factors of *K* and *D* for permeation across HMS SC were to be determined using the stripped HMS data and the two-layer skin model.

2.2. Materials

Hairless mice (strain SKH-HR1, 10–12 weeks old) were obtained from Charles River (Wilmington, MA). The following were the materials used in the present study and their suppliers: 1-octyl-2-pyrrolidone (OP), ISP Technologies Inc. (Wayne, NJ); ^{3}H-corticosterone (^{3}H-CS) and ^{3}H-estradiol (^{3}H-E2β), NEN Life Science Products (Boston, MA); ^{3}H-raffinose, American Radiolabeled Chemicals (St. Louis, MO); methanol (HPLC grade), Aldrich Co. (Milwaukee, WI); ethanol (100% purity, EtOH), AAPER Alcohol and Chemical Co. (Shelbyville, Kentucky); heptane (HPLC grade), EM Science Co. (Darmstadt, Germany); CS and E2β, Sigma Chemical (St. Louis, MO). The purity of the ^{3}H-CS and ^{3}H-E2β was checked to be >95%. 1-Hexyl-2-azacycloheptanone (HAZ) was synthesized at the Chemical Synthesis Facility, University of Utah (Salt Lake City, UT). PBS solution was prepared from phosphate buffered saline (PBS) tablets (Sigma Co, St. Louis, MO) and deionized distilled water.

2.3. HMS permeability experiments with ^{3}H-CS

Full-thickness or stripped HMS permeability experiments with ^{3}H-CS were carried out as previously described (Yoneto et al., 1995) in a two-chamber diffusion cell (each chamber had a 2-ml volume and an effective diffusion area of around 0.7 cm^2). Briefly, these experiments involve a protocol to equilibrate the enhancer solution with the HMS before the start of the transport experiments. The main differences in the present experiments from those described previously were the following. First, the protocol of withdrawing samples from the receiver chamber was carefully designed to maintain sink conditions in the chamber to obtain adequate non-steady-state and steady-state transport data. Specifically, samples were withdrawn from the receiver chamber every 40 min for full-thickness HMS and 30 min for stripped HMS in PBS. In the presence of enhancers (OP or HAZ), samples were withdrawn from the receiver chamber every 30 min for full-thickness HMS and 15 min for stripped HMS. In transport experiments with stripped HMS, the permeant solution in the donor chamber was also frequently replaced by fresh donor solution to maintain a constant permeant concentration on the donor side throughout the transport experiments. The samples from both donor and receiver chambers were then mixed with 10 ml of scintillation cocktail (Ultima Gold, Packard Instrument Company, Meriden, CT) and analyzed with a liquid scintillation counter (Packard TriCarb Model 1900 TR Liquid Scintillation Analyzer).

The total steady-state permeability coefficient for full-thickness skin (P_T) and the permeability coefficient for viable epidermis–dermis combination ($P_{D/E}$) of the probe permeants were calculated according to the following equation:

$$P_T \text{ and } P_{D/E} = \frac{1}{AC_D}\frac{dQ}{dt} \quad (1)$$

where A is the effective diffusion area of the diffusion cell, C_D is the concentration in the donor chamber and (dQ/dt) is the slope of the steady-state region of the plot of the cumulative amount of permeant transported into the receiver chamber versus time. Experiments were run long enough so that the "steady-state" regions were typically around three to five times longer than the lag times. The enhancement factor (E) of the steady-state permeability coefficients (P_{SC}) for the SC lipoidal pathway were determined as previously described (Ghanem et al., 1987, 1992; Kim et al., 1992).

2.4. Inhibition of ^{3}H-CS metabolism and ^{3}H-CS purity check in the transport experiments

It was found in preliminary experiments that a small percentage of ^{3}H-CS could be metabolized by enzymes existing in HMS (data not shown). This finding is consistent with the previous findings of catabolic enzymes in the viable epidermis layer of HMS (Liu, 1989; Chantasart et al., 2004). In order to inhibit the metabolism, cold CS (around 0.2 mg/ml) was used in the transport experiments with ^{3}H-CS, and the purity of ^{3}H-CS was checked at different time points (2, 4 and 6 h) during the experiment to monitor possible metabolism of CS. The ^{3}H-CS samples from the donor and receiver chambers were then assayed with an HPLC system (Hewlett Packard, Santa Clarita, CA) and the liquid scintillation counter.

2.5. HMS permeability experiments with ^{3}H-E2β and ^{3}H-CS in the presence of 2% EtOH

As explained in Section 2.1, CS was chosen as the surrogate permeant for E2β because preliminary transport experiments with E2β showed significant metabolism of the compound in HMS. In order to compare the results of the model analysis of CS in the present study and the partition enhancement results of E2β obtained in the previous study (He et al., 2003), it was first necessary to compare the steady-state transport enhancement of both CS and E2β in the presence of the studied chemical permeation enhancers (OP and HAZ) under conditions where the metabolism of E2β could be mostly inhibited. Preliminary experiments showed that E2β metabolism could be significantly inhibited in the presence of 2% ethanol. Under this condition, less than 10% ^{3}H-E2β was metabolized and recovered in the receiver chamber throughout the transport experiments, and such extent of metabolism was believed to have negligible influence on the steady-state permeability coefficient of E2β (Liu, 1989). Furthermore, 2% ethanol in the system was shown not to have any observable enhancement effects on E2β transport across the lipoidal pathway of HMS SC (Liu, 1989). Based on these previous results, transport experiments were conducted with both ^{3}H-E2β and ^{3}H-CS in the presence of 2% ethanol in PBS and in the enhancer solutions (OP or HAZ).

The transport experiments with ^{3}H-E2β and ^{3}H-CS were conducted in the same way as described in Section 2.3 except that samples from the receiver chamber were withdrawn every 40 min for full-thickness HMS and every 20 min for stripped HMS to maintain sink conditions in the receiver chamber. One milliliter of the permeant solution in the donor chamber was refreshed every 40 min for full-thickness HMS and every 20 min for stripped HMS to maintain a constant concentration in the donor chamber. The steady-state permeability coefficients of ^{3}H-CS and ^{3}H-E2β were determined according to Eq. (1) and the enhancement factors were calculated as previously described (Ghanem et al., 1987, 1992; Kim et al., 1992).

2.6. Data analysis with the one-layer skin transport model

The simplest model for skin transport is a one-layer model based on the assumption that the skin is a single homogeneous layer. An analytical solution for the amount of permeant transport through skin derived from Fick's law is shown in Eq. (2) (Okamoto et al., 1988):

$$Q_t = AK'C_0 \left[D't - \frac{1}{6} - \frac{2}{\pi^2} \sum_{1}^{250} \frac{(-1)^n}{n^2} \times \exp(-D'n^2\pi^2 t) \right]$$

$$D' = \frac{D}{L^2}, \qquad K' = KL, \qquad P = D'K' \tag{2}$$

where Q_t is the total amount of permeant transport through skin; A the effective diffusion area; L the effective diffusion length; D the diffusion coefficient; K the partition coefficient; C_0 the constant concentration of permeant at the donor chamber; t the time; P the permeability coefficient.

The two reduced parameters K' and D' in Eq. (2) were defined in order to minimize the number of parameters for least squares fitting in the model analysis of the experimental transport data. The use of parameters K' and D' avoids the uncertainties in assigning the L value; it is difficult to assign a value to the effective path length (L) across SC (Talreja et al., 2001). Enhancement factors of K for HMS ($E_{K,\mathrm{HMS}}$) and D

for HMS ($E_{D,\mathrm{HMS}}$) were determined based on K' and D' according to the following equations:

$$E_{D,\mathrm{HMS}} = \frac{D_{\mathrm{enhancer}}}{D_{\mathrm{PBS}}} = \frac{D'_{\mathrm{enhancer}}}{D'_{\mathrm{PBS}}} \quad (3)$$

$$E_{K,\mathrm{HMS}} = \frac{K_{\mathrm{enhancer}}}{K_{\mathrm{PBS}}} = \frac{K'_{\mathrm{enhancer}}}{K'_{\mathrm{PBS}}} \quad (4)$$

where subscripts enhancer and PBS refer to enhancer solution and PBS conditions, respectively.

It is assumed in the present study that the L value is constant in PBS and in the presence of the enhancers for the permeation of lipophilic permeants such as CS and E2β. This assumption is consistent with the finding by Yu et al. (2001).

2.7. Characterization of the combined dermis and viable epidermis (D/E) layer of HMS: partition experiments of raffinose and CS with stripped HMS

Stripped HMS was prepared as described previously (Yoneto et al., 1995). A portion of the stripped HMS (~0.1 g) was sandwiched between two hemacytometer cover glasses (Scientific Products, McGaw Park, IL) and its thickness was measured with micrometer calipers. The stripped HMS was then weighed and equilibrated in 10 ml PBS or enhancer/PBS solution with appropriate amount of ^{3}H-CS or ^{3}H-raffinose for 3 h. The 3 h time point was chosen according to time-dependent preliminary data at 1 and 3 h. After equilibration, the membrane was taken out of the solution with tweezers and blotted on Kimwipes® tissue paper. The thickness of the stripped HMS was measured again after equilibration. The wet, stripped HMS was then weighed, and the content was extracted in either 6 ml of EtOH or PBS for ^{3}H-CS or ^{3}H-raffinose, respectively. The extraction time was 6h, determined by preliminary time-dependent data at 1, 2, 6, and 20 h for ^{3}H-CS and ^{3}H-raffinose. After the first extraction, the stripped HMS was transferred into another 6 ml EtOH or PBS for the second extraction to check the completeness of the first extraction. The amount of ^{3}H-CS or ^{3}H-raffinose in the extraction solution was determined by the liquid scintillation counter, and the porosity (ε) and binding constant (R) of D/E were calculated according to the following equation:

$$C_{\mathrm{T}} = \varepsilon(1 + R)C_{\mathrm{P}} \quad (5)$$

where C_{T} is the total concentration of ^{3}H-CS or ^{3}H-raffinose in D/E and C_{P} is the concentration of ^{3}H-CS or ^{3}H-raffinose in the aqueous compartment of D/E. It is assumed that the binding constant is zero ($R = 0$) for raffinose; this permits calculating ε from the ^{3}H-raffinose C_{T} value and then R for ^{3}H-CS from its C_{T} value.

2.8. Characterization of D/E of HMS: determination of membrane tortuosity

The lag time ($t_{\mathrm{lag,D/E}}$) for ^{3}H-CS transport across the D/E layer was determined in permeation experiments with stripped HMS by extrapolating the steady-state slope of ^{3}H-CS permeation data to the time-axis in cumulative amount versus time plots. The tortuosity values of D/E were calculated according to the following equations:

$$K_{\mathrm{D/E}} = \varepsilon(1 + R) \quad (6)$$

$$P_{\mathrm{D/E}} = K_{\mathrm{D/E}} \frac{D_{\mathrm{D/E}}}{L_{\mathrm{D/E}}} \quad (7)$$

$$t_{\mathrm{lag,D/E}} = \frac{L^2_{\mathrm{D/E}}}{6D_{\mathrm{D/E}}} = \frac{h_{\mathrm{D/E}}\tau_{\mathrm{D/E}}(1 + R)\varepsilon}{6P_{\mathrm{D/E}}} \quad (8)$$

$$L_{\mathrm{D/E}} = \tau_{\mathrm{D/E}} h_{\mathrm{D/E}} \quad (9)$$

where $K_{\mathrm{D/E}}$ is the partition coefficient of CS for D/E calculated from ε and R of D/E for CS obtained in the previous section. $P_{\mathrm{D/E}}$ is the steady-state permeability coefficient of CS across stripped HMS. $L_{\mathrm{D/E}}$ is the effective diffusion path length of CS through D/E, which equals the product of the D/E thickness ($h_{\mathrm{D/E}}$) and tortuosity ($\tau_{\mathrm{D/E}}$).

2.9. Data analysis with the two-layer skin transport model

A two-layer numerical skin transport model was developed for the study of permeant transporting across the SC and D/E (Fig. 1). This model divides the SC and D/E into a number of layers characterized by partition, diffusion, and dimension parameters. A hypothetical aqueous interface layer was created between the SC and D/E layers (Fig. 1) with a concentration of C_i to account for the instantaneous equilibrium between SC and D/E at the interface. The permeant concentration in the donor chamber was assumed constant, which was true in all transport experiments carried out in

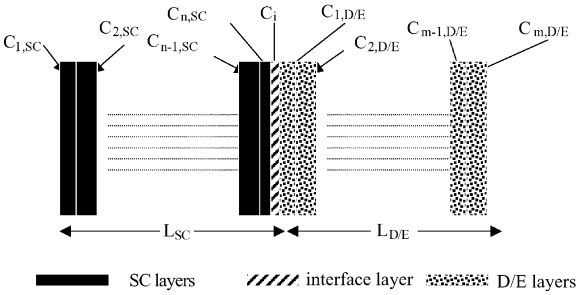

Fig. 1. Scheme for the two-layer skin model.

the present study. The receiver chamber concentration was kept at sink conditions. The transport data of full-thickness HMS was analyzed with a least squares fitting software Scientist (MicroMath, Salt Lake City, UT) using the two-layer transport model to obtain partition coefficient (K_{SC}) and diffusion coefficient (D_{SC}) of SC. K'_{SC} and D'_{SC} of SC were then calculated according to the definitions of K' and D' in Eq. (2): $K'_{SC} = K_{SC}L_{SC}$; $D'_{SC} = D_{SC}/L^2_{SC}$. The enhancement of K'_{SC} and D'_{SC} ($E_{K,SC}$ and $E_{D,SC}$, respectively) was calculated according to Eqs. (3) and (4).

The equations for the two-layer skin model employed in the model calculations are given below with symbols indicated in Fig. 1:

$$\frac{dC_{1,SC}}{dt} = \frac{p_1[2(K_{SC}C_D - C_{1,SC}) - (C_{1,SC} - C_{2,SC})]}{x_1},$$

$$\frac{dC_{2,SC}}{dt} = \frac{p_1[C_{1,SC} - 2C_{2,SC} - C_{3,SC}]}{x_1},$$

$$\ldots, \frac{dC_{n,SC}}{dt} = \frac{p_1[(C_{n-1,SC} - C_{n,SC}) - 2(C_{n,SC} - C_iK_{SC})]}{x_1},$$

$$C_i = \frac{p_1C_{n,SC} + p_2C_{1,D/E}}{p_2K_{D/E} + p_1K_{SC}},$$

$$\frac{dC_{1,D/E}}{dt} = \frac{p_2[2(C_iK_{D/E} - C_{1,D/E}) - (C_{1,D/E} - C_{2,D/E})]}{x_2\varepsilon(1+R)},$$

$$\frac{dC_{2,D/E}}{dt} = \frac{p_2[C_{1,D/E} - 2C_{2,D/E} - C_{3,D/E}]}{x_2\varepsilon(1+R)},$$

$$\ldots, \frac{dC_{m,D/E}}{dt} = \frac{p_2[(C_{m-1,D/E} - C_{m,D/E}) - 2(C_{m,D/E} - K_{D/E}C_R)]}{x_2\varepsilon(1+R)},$$

$$\frac{dQ_R}{dt} = 2p_2A(C_{m,D/E} - C_R) \quad (10)$$

where t is the time; D_{SC} the diffusivity in SC; K_{SC} the partition coefficient of SC; L_{SC} the effective diffusion pathway length in SC; $x_1 = L_{SC}/n$ representing diffusion path length in each SC layer; $p_1 = D_{SC}/x_1$, representing permeation coefficient of each SC layer; ε the porosity of D/E; R the binding constant of CS in the D/E; $\tau_{D/E}$ the tortuosity in D/E; $h_{D/E}$ the thickness of D/E; $L_{D/E} = h_2\tau_{D/E}$ the effective diffusion path length of CS across each D/E layer; $x_2 = L_{D/E}/m$, representing diffusion path length in each D/E layer; $p_2 = P_{D/E}m$, representing permeation coefficient of each D/E layer; A the effective surface area; Q_R the cumulative amount of permeant in the receiver chamber; V_D, V_R the volume of the donor and receiver chambers, respectively; C_D the concentration in the donor chamber which is kept constant; C_R the concentration in the receiver chamber which is assigned a zero value; $C_{1,SC}$ to $C_{n,SC}$ the concentration of CS in the middle position of each SC layer; $C_{1,D/E}$ to $C_{m,D/E}$ the concentration of CS in the middle position of each D/E layer; C_i the concentration of CS in the interface layer.

To test the number of layers of SC required to obtain accurate results with the skin transport model, K'_{SC} and D'_{SC} values were determined with different numbers of layers of SC when the number of layers of D/E was kept constant at 20. The results showed that when the number of layers of SC was equal to or above 16, the values of K'_{SC} and D'_{SC} were converged (Figs. 2 and 3). Similar results were found with the analysis of K'_{SC} and D'_{SC} when different numbers of layers of D/E were used and the number of SC layers was kept constant at 20. Based on these results, it was determined that when SC was divided into 20 layers and D/E was divided into 20 layers in the two-layer skin transport model for the least squares fitting analysis, the numbers of layers

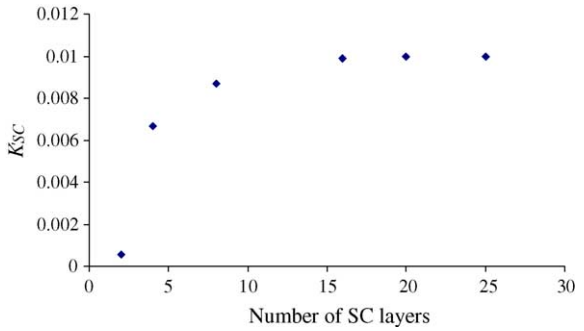

Fig. 2. K'_{SC} vs. number of SC layers in the two-layer model when the number of D/E layers is fixed at 20.

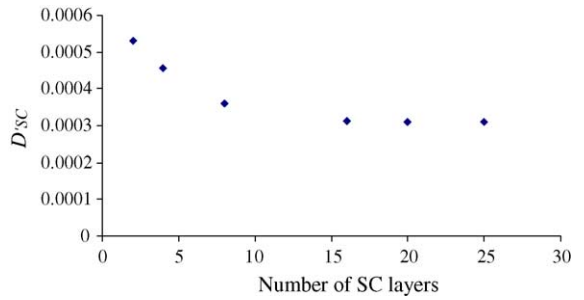

Fig. 3. D'_{SC} vs. number of SC layers in the two-layer model when the number of D/E layers is fixed at 20.

were large enough to mimic permeation across SC and D/E. Different values of the SC diffusion path length were also used to test the influence of L_{SC} on K'_{SC} and D'_{SC} in the two-layer skin model analysis. In this analysis, the L_{SC} value was varied from 0.003 to 2.0 cm.

3. Results

3.1. Permeation and purity check data of ^{3}H-CS in transport experiments with HMS

The permeability coefficients and enhancement factors of CS across full-thickness and stripped HMS in PBS and enhancer solutions were calculated as described previously (Ghanem et al., 1987, 1992; Kim et al., 1992). Table 1 presents the results of the permeability coefficients and enhancement factors in the present study. First, as can be seen from these data, the solubility correction of CS in the presence of OP and HAZ is negligible. Second, the enhancement

Table 1
Steady-state corticosterone (CS) permeability coefficients and the purity of ^{3}H-CS for the permeation experiments with HMS

Solution	P_T (10^{-6} cm/s)[a]	$P_{D/E}$ (10^{-6} cm/s)[a]	P_{SC} (10^{-6} cm/s)[a]	S_X/S_0[b]	E[c]	Purity of ^{3}H-CS at receiver chamber (%)[d]	Purity of ^{3}H-CS at donor chamber (%)[d]	Purity of stock ^{3}H-CS (%)[e]
PBS	0.29 ± 0.05	34 ± 5	0.29 ± 0.06	–	–	97 ± 1	98 ± 1	98 ± 1
OP (2.0 mM)	3.2 ± 0.9	50 ± 10	3.4 ± 1.2	1.0	11.8 ± 4.4	98 ± 2	98 ± 1	98 ± 1
HAZ (4.3 mM)	3.1 ± 0.5	55 ± 8	3.3 ± 0.7	1.0	11.5 ± 3.3	99 ± 1	99 ± 1	98 ± 1

[a] Mean ± S.D. ($n \geq 3$).
[b] Solubility ratio: (CS solubility in enhancer solution, S_X)/(CS solubility in PBS, S_0); S_X/S_0 corrects for any activity coefficient differences between the activity coefficient in PBS and that in the enhancer solution.
[c] Enhancement factor, $E = (P_{SC,X}/P_{SC,0})(S_X/S_0)$, where subscripts X and 0 are enhancer solution and PBS conditions, respectively (Ghanem et al., 1987; Kim et al., 1992).
[d] Average percent of purity obtained at different time points during the permeation experiments.
[e] Average percent of purity obtained on different days.

Table 2
Steady-state permeability coefficients of ^{3}H-E2β and ^{3}H-CS with full-thickness HMS and stripped HMS in the presence of 2% ethanol

Solution	P_T (10^{-6} cm/s)[a]	$P_{D/E}$ (10^{-6} cm/s)[a]	P_{SC} (10^{-6} cm/s)[a]	S_X/S_0[b]	E[c]
Transport experiments with ^{3}H-E2β in the presence of 2% ethanol					
PBS (2% ethanol)	5.3 ± 0.6	49 ± 5	6.0 ± 0.9	–	–
OP (2.0 mM + 2% ethanol)	18 ± 5	33 ± 15	39 ± 20	1.3	8.5 ± 4.6
HAZ (4.3 mM + 2% ethanol)	15 ± 5	32 ± 14	28 ± 15	1.4	6.5 ± 3.5
Transport experiments with ^{3}H-CS in the presence of 2% ethanol					
PBS (2% ethanol)	0.24 ± 0.03	43 ± 9	0.24 ± 0.06	–	–
OP (2.0 mM + 2% ethanol)	1.7 ± 0.6	40 ± 3	2.0 ± 0.7	1.1	8.1 ± 3.0
HAZ (4.3 mM + 2% ethanol)	1.5 ± 0.5	37 ± 2	1.6 ± 0.5	1.2	7.7 ± 2.5

[a] Mean ± S.D. ($n \geq 3$).
[b] Solubility ratio: (CS solubility in enhancer solution, S_X)/(CS solubility in PBS, S_0).
[c] Enhancement factor; see Table 1, footnote c.

factors of CS transport across HMS are 11.8 and 11.5 when the enhancer concentrations are 2.0 and 4.3 mM for OP and HAZ, respectively. These data are consistent with the results of previous enhancer studies (He et al., 2003; Warner et al., 2003). Also shown in Table 1 are the purity check data of ^{3}H-CS (last three columns in Table 1). The purity of ^{3}H-CS in both donor and receiver chambers was checked throughout the transport experiments (2, 4, 6 or 7.5 h). The purity of the stock ^{3}H-CS was also determined and shown in Table 1 as reference. These data indicate negligible ^{3}H-CS metabolite and impurity.

3.2. Permeation data of ^{3}H-E2β and ^{3}H-CS with HMS in the presence of 2% ethanol

The steady-state permeability coefficients of ^{3}H-E2β and ^{3}H-CS in the presence of 2% ethanol in PBS and the enhancer solutions with both full-thickness and stripped HMS are shown in Table 2. As expected, CS permeation across HMS was SC-controlled; $P_{D/E}$ was about 20–200 times higher than P_T for ^{3}H-CS in PBS or in the enhancer solutions. However, the $P_{D/E}$ values were only 2–10 times higher than P_T for ^{3}H-E2β under the same conditions, indicating that E2β permeation was approaching D/E controlled. Despite this difference, when the P_{SC} values were delineated in the assessment of permeation enhancement induced by the chemical permeation enhancers (OP or HAZ), the enhancement factors (the last column of Table 2) for ^{3}H-E2β and ^{3}H-CS were essentially the same under these conditions. These enhancement factor data suggest similar permeation enhancement mechanisms of the enhancers (OP and HAZ) for the lipophilic model permeants E2β and CS. A similar conclusion was drawn in a previous study (Yoneto et al., 1995). This finding enables us to compare the results of the transport model analysis using CS in the present study and the results obtained in the previous equilibrium partitioning study using E2β (He et al., 2003, 2004).

3.3. Data analysis with the one-layer skin transport model

The transport data of ^{3}H-CS across full-thickness HMS were analyzed by the one-layer skin transport model (Eq. (2)). K' and D' were obtained with least squares fitting of the data and then used to determine $E_{K,HMS}$ and $E_{D,HMS}$ (Eqs. (3) and (4)). The least squares fittings are generally satisfactory with the one-layer

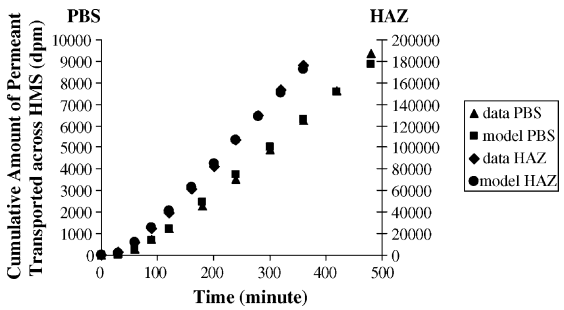

Fig. 4. Experimental transport data and model fitting analysis with the one-layer skin model ($K' = 6.2 \times 10^{-3}$ and 57×10^{-3} cm, $D' = 4.2 \times 10^{-5}$ and 6.1×10^{-5} s^{-1} for PBS and 4.3 mM HAZ, respectively). Symbols: triangles, experimental data PBS; squares, model fitting PBS; diamonds, experimental data HAZ; circles, model fitting HAZ.

Table 3
Enhancement factors of partition coefficient ($E_{K,HMS}$) and diffusion coefficient ($E_{D,HMS}$) for ^{3}H-CS transport across HMS obtained with the one-layer skin model and $E_{K,SC}$ and $E_{D,SC}$ obtained with the two-layer skin model

Solution	One-layer skin model[b]				Two-layer skin model			
	K' (10^{-3} cm)	D' (10^{-5} s^{-1})	$E_{K,HMS}$	$E_{D,HMS}$	K'_{SC} (10^{-3} cm)	D'_{SC} (10^{-4} s^{-1})	$E_{K,SC}$	$E_{D,SC}$
PBS	6.4 ± 0.4[c]	4.0 ± 0.3[c]	–	–	1.2 ± 0.3[c]	2.5 ± 0.8[c]	–	–
OP (2.0 mM)[a]	38 ± 3[c]	7.7 ± 1.7[c]	5.9 ± 0.6	1.9 ± 0.4	7.0 ± 1.0[c]	4.6 ± 1.9[c]	6.0 ± 1.9	1.8 ± 0.9
HAZ (4.3 mM)[a]	46 ± 10[c]	6.5 ± 1.3 [c]	7.2 ± 1.5	1.6 ± 0.3	9.2 ± 1.8[c]	3.2 ± 1.0[c]	7.9 ± 2.8	1.3 ± 0.6

[a] Agueous concentrations of OP and HAZ that induced $E \simeq 11$.
[b] Mean ± S.D. ($n \geq 3$).
[c] One-layer model and two-layer model values are significantly different ($p < 0.05$).

model. Representative least squares fittings of the transport data are shown in Fig. 4 for the PBS and HAZ conditions (4.3 mM). The average values of K', D', $E_{K,HMS}$ and $E_{D,HMS}$ are shown in Table 3. The data show that the enhancement of permeant partitioning into the transport rate-limiting domain of HMS is significantly higher than the enhancement of permeant diffusion in the domain ($p < 0.05$, t-test). When the total flux enhancement (E) was 11.8 for OP, $E_{K,HMS}$ was 5.9 and $E_{D,HMS}$ was 1.9. For HAZ with E of 11.5, $E_{K,HMS}$ was 7.2 and $E_{D,HMS}$ was 1.6. This suggests that the transport enhancement of CS across HMS was mainly driven by partition enhancement in the rate-limiting domain of HMS. The data also show essentially the same enhancement values ($E_{K,HMS}$ and $E_{D,HMS}$) for both enhancers (OP and HAZ) under the isoenhancement conditions of $E \simeq 11$. This is consistent with our hypotheses of the mechanism of action of permeation enhancers discussed in previous and present studies (Yoneto et al., 1995; Warner et al., 2003; Chantasart et al., 2004; He et al., 2004).

3.4. Parameters for D/E

As described in the experimental section, the porosity (ε) of D/E was determined from the ^{3}H-raffinose data with Eq. (5) assuming the binding constant $R = 0$, and it was found that the ε values were essentially constant with and without the presence of the enhancers, $\varepsilon = 0.64 \pm 0.02$. The R values of CS for D/E were then determined using Eqs. (5) and (6) and the ^{3}H-CS partitioning data. From the transport lag time of CS with stripped HMS, the tortuosity values ($\tau_{D/E}$) of the diffusion path of D/E for CS were also determined using Eqs. (6)–(9). These results are summarized in Table 4. As can be seen in the table, the R values increased approximately 30% and the tortuosity values decreased approximately three times in the presence of the enhancers. These D/E parameters (ε, R and $\tau_{D/E}$) were then used in the two-layer model analysis below.

3.5. Data analysis with the two-layer skin transport model

The two-layer transport model was applied to each set of the CS transport data to obtain the least squares-fitting K'_{SC} and D'_{SC} of CS in PBS, OP (2.0 mM), and HAZ (4.3 mM). Representative least squares fittings of the transport data with the two-layer model are shown in Fig. 5 for the PBS and HAZ conditions. As shown in Fig. 5, the least squares fittings were satisfactory

Table 4
Parameters for D/E layer of HMS[a]

Solution	$P_{D/E}$ (10^{-6} cm/s)	Lag time (min)	R[b]	$\tau_{D/E}$[c]
PBS	34 ± 5	34 ± 9	3.6 ± 0.1	7.2 ± 2.6
OP (2.0 mM)	50 ± 10	7 ± 4	4.5 ± 0.2	2.3 ± 1.1
HAZ (4.3 mM)	55 ± 8	9 ± 6	4.3 ± 0.4	2.4 ± 1.3

[a] Mean ± S.D. ($n \geq 3$).
[b] Determined using porosity (ε) of 0.64 (see Section 3.4).
[c] Thickness of D/E ($h_{D/E}$) was in the range from 0.018 to 0.023 cm.

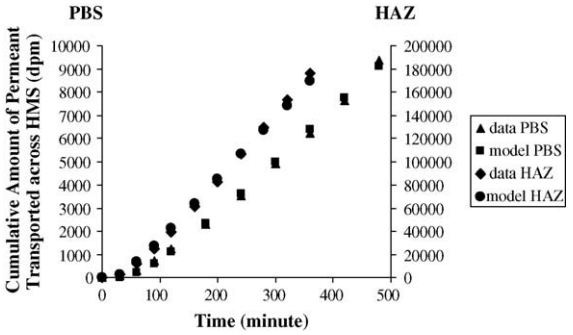

Fig. 5. Experimental transport data and model fitting analysis with two-layer skin model ($K'_{SC} = 0.9 \times 10^{-3}$ and 9.1×10^{-3} cm, $D'_{SC} = 3.1 \times 10^{-4}$ and 3.8×10^{-4} s^{-1} for PBS and 4.3 mM HAZ, respectively). Symbols: triangles, experimental data PBS; squares, model fitting PBS; diamonds, experimental data HAZ; circles, model fitting HAZ.

with the two-layer skin models. The average values of K'_{SC}, D'_{SC}, $E_{K,SC}$ and $E_{D,SC}$ obtained with the two-layer model are shown in Table 3, and the $E_{K,SC}$ and $E_{D,SC}$ data again show significantly higher permeant partitioning enhancement into the transport rate-limiting domain of HMS than the enhancement of permeant diffusion in the domain ($p < 0.05$, t-test). Although the absolute values of K'_{SC} and D'_{SC} obtained by the two-layer model analysis are different from those obtained with the one-layer model, $E_{K,SC}$ and $E_{D,SC}$ values for both OP and HAZ are essentially the same as $E_{K,HMS}$ and $E_{D,HMS}$ obtained with the one-layer model (Table 3), respectively.

To test the influence of L_{SC} on the K'_{SC} and D'_{SC} results, L_{SC} value was varied in one set of the transport data (in 4.3 mM HAZ). The results are shown in Table 5. The K'_{SC} and D'_{SC} values obtained using the two-layer skin transport model are seen to be independent of the value of L_{SC}.

Table 5
K'_{SC} and D'_{SC} obtained with the two-layer model with different L_{SC} values obtained from one transport data of CS in 4.3 mM HAZ solution

L_{SC} (cm)	K'_{SC} (10^{-2} cm)	D'_{SC} (10^{-4} s^{-1})
0.003	1.00	3.10
0.0127	1.00	3.10
1.0	0.97	3.19
2.0	0.98	3.15

4. Discussion

4.1. Correlation between the enhancement of partitioning in the transport rate-limiting domain and that in the intercellular lipid domain of HMS SC

Previous studies with chemical permeation enhancers (Warner et al., 2003; Chantasart et al., 2004; He et al., 2004) have suggested that the microenvironment of the enhancer site of action and the macroscopic SC intercellular lipid "phase" are both well represented by (water-saturated) liquid *n*-octanol. It was also found in these previous partitioning experiments that the partitioning enhancement of E2β with the intercellular lipids of HMS SC was in the range of 5–7 under the isoenhancement conditions of $E = 10$ for the enhancers studied. A significant finding in the present study is that the partition coefficient enhancement of permeants deduced from the model analyses of relevant HMS SC transport data was in the range of 6–8 when the total (transport) enhancement was around 11, which is remarkably consistent with the partition coefficient enhancement of permeants obtained from the equilibrium partitioning experiment with HMS SC in the previous studies. This finding provides quantitative evidence that the rate-limiting domain for the transport of the model permeants through the lipoidal pathway of HMS SC and the intercellular lipid "phase" probed in the equilibrium partitioning experiments have similar properties regarding the partitioning enhancement effects of chemical permeation enhancers upon lipophilic model permeants and that these domains are also very likely to be the same.

It is worthwhile to point out that similar lag time reduction for CS across HMS were also observed for all the permeation enhancers studied to date under the isoenhancement conditions of $E = 10$ (the *n*-alkyl enhancers, branched alkanols, and enhancers with a carbon–carbon double bond in their alkyl chains; Warner et al., 2003; Chantasart et al., 2004; He et al., 2004). Although the same model analysis could not be performed rigorously using these previous data due to the different experimental designs employed in the present and previous studies, the steady-state permeability and lag time data of CS with these enhancers (unpublished data) suggest the same conclusion can be applied to all enhancers studied to date in our

laboratory; i.e., total flux enhancement of lipophilic permeants across HMS is mainly driven by enhancing the partitioning of the permeant into the rate-limiting domain and to a lesser extent by enhancing diffusion coefficients.

4.2. Physico-chemical interpretation of transport enhancement of lipophilic permeant in HMS induced by chemical permeation enhancers

Model analyses based on the Fick's diffusion theory enable us to elucidate the influence of chemical permeation enhancers on the permeation of drug molecules across HMS in terms of partition and diffusion coefficient enhancement for quantitative study of the mechanism of transdermal permeation enhancement. Efforts have been made in the analysis of drug penetration profiles in the presence of chemical permeation enhancers (Yamashita et al., 1993), and it has been reported that drug partitioning into skin increased but the diffusivities in skin were relatively unaffected by chemical permeation enhancers during transdermal transport. The technique of two-photon fluorescence microscopy has also been applied to obtain the enhancement of K and D induced by chemical permeation enhancers in model compound permeation across full-thickness human cadaver skin (Yu et al., 2001), and it has been reported that the permeability enhancement was primarily caused by an increase in the skin partition coefficient.

It has been generally difficult to obtain quantitative partition and diffusion data for permeation across SC because of limitations related to the quality of the data. The present transport experiments were conducted in a manner to avoid artifacts, such as by maintaining a constant donor concentration and receiver sink conditions and minimizing possible interference of metabolism and impurities. The results of the present transport study suggest that the transport enhancement of lipophilic permeants CS and E2β across HMS is mainly driven by enhancement of permeant partitioning into the rate-limiting domain of HMS. Because the intercellular lipids have been suggested to be the main pathway for the permeation of lipophilic compounds such as CS and E2β (Bouwstra et al., 2000), the relatively high partition coefficient enhancement found in the present study suggests either alterations of the polarity and/or the free volume of the chemical environment of the SC intercellular lipid lamellae. Previous studies (Anderson et al., 1988; Raykar et al., 1988; Anderson and Raykar, 1989) have shown that the microenvironment of the rate-limiting domains for steroidal permeant transport across SC in buffered saline can be well modeled by the octanol liquid phase. Recently, work in our laboratory (Warner et al., 2003; Chantasart et al., 2004; He et al., 2004) has demonstrated correlations between permeant transport across SC, the partitioning of chemical permeation enhancers into the intercellular lipids of SC, and the partitioning of the permeants into SC for more than 30 permeation enhancers of different molecular sizes. The results of these recent enhancer studies furthermore suggest that the microenvironment involved in the action of permeation enhancement in HMS SC is similar to water-saturated liquid *n*-octanol. Together, these results indicate that the microenvironment of the transport rate-limiting domains in HMS SC behaves like liquid *n*-octanol in the presence of and in the absence of the studied permeation enhancers, and that the enhancers do not significantly alter the polarity of the microenvironment in the stratum corneum transport rate-limiting domain. It is then logical to suggest that the permeation enhancers act only by increasing the free volume and decreasing the microviscosity of the SC lipid lamellae to enhance permeant partitioning into the lipid lamellae. This hypothesis is consistent with previous fluorescence studies with SC lipid liposomes (Yoneto et al., 1996). It is interesting that the chemical permeation enhancers do not greatly enhance permeant diffusion in the SC intercellular lipids (the enhancement of diffusion coefficient was around 1.3–1.9), which is expected if the free volume of the lipid lamellae has been increased (Xiang and Anderson, 1998) under these experimental conditions. This requires further investigation of the relationship between SC lipid lamellae fluidization and permeant partitioning into and its diffusivity in SC lipid lamellae.

4.3. One-layer and two-layer skin models in HMS transport studies

Because the SC is considered the primary transdermal transport barrier for most permeants, some previous studies have been based on the assumption that full-thickness skin is a homogeneous one-layer membrane (SC only) to simplify the analysis of transport data obtained with full-thickness skin (Foreman and Kelly, 1976; Hashida et al., 1988; Okamoto et al., 1988,

1991). A more rigorous approach has been to consider full-thickness skin as a two-layer (SC and D/E) membrane (Tojo et al., 1987; Tojo, 1988; Okamoto et al., 1989; Yamashita et al., 1994, 1995). In the present study, the enhancement effects of chemical permeation enhancers on permeant partition and diffusion coefficients were analyzed by both the one-layer and two-layer models. A first impression of the similar enhancement of K and D obtained in the one-layer ($E_{K,\mathrm{HMS}}$ and $E_{D,\mathrm{HMS}}$) and two-layer ($E_{K,\mathrm{SC}}$ and $E_{D,\mathrm{SC}}$) skin transport models (Table 3) is that the one-layer skin model may be adequate for the purpose of studying the enhancement effects of permeation enhancers upon the permeation of lipophilic permeants (e.g., CS) across SC. However, as shown in Table 3, the K' and D' values are different in the one-layer and two-layer model analyses (t-test, $p < 0.05$ in all comparisons). The different K' and D' values obtained from the one-layer and two-layer models imply that the similar enhancement values obtained in the one-layer and two-layer model analyses may be somewhat fortuitous. Although the steady-state permeation of CS across HMS is mainly SC-controlled (Warner et al., 2001; He et al., 2003), permeant binding to the D/E (Table 4) can significantly alter the early-time (non-steady-state) transport profile of the lipophilic permeant. Such effects have been tested in hypothetical model simulations with Eq. (10) (unpublished data); e.g., when D/E was removed in the model simulation, the time to establish the steady-state concentration profile and transport lag time decrease. Therefore, caution must be exercised in the interpretation of full-thickness skin transport data using a one-layer homogeneous skin transport model that ignores the D/E layer.

Acknowledgements

The authors thank Dr. Abdel-Halim Ghanem and Dr. Doungdaw Chantasart for their help. This work was supported in part by NIH Grant GM 063559.

References

Anderson, B.D., Higuchi, W.I., Raykar, P.V., 1988. Heterogeneity effects on permeability–partition coefficient relationships in human stratum corneum. Pharm. Res. 5, 566–573.

Anderson, B.D., Raykar, P.V., 1989. Solute structure–permeability relationships in human stratum corneum. J. Invest. Dermatol. 93, 280–286.

Bouwstra, J.A., Dubbelaar, F.E.R., Gooris, G.S., Ponec, M., 2000. The lipid organisation in the skin barrier. Acta Derm. Venereol. Suppl. 208, 23–30.

Chantasart, D., Li, S.K., He, N., Warner, K.S., Prakongpan, S., Higuchi, W.I., 2004. Mechanistic studies of branched-chain alkanols as skin permeation enhancers. J. Pharm. Sci. 93, 762–779.

Foreman, M.I., Kelly, I., 1976. The diffusion of nandrolone through hydrated human cadaver skin. Br. J. Dermatol. 95, 265–270.

Ghanem, A.H., Mahmoud, H., Higuchi, W.I., Rohr, U.D., Borsadia, S., Liu, P., Fox, J.L., Good, W.R., 1987. The effects of ethanol on the transport of estradiol and other permeants in hairless mouse skin. II. A new quantitative approach. J. Contr. Release 6, 75–83.

Ghanem, A.H., Mahmoud, H., Higuchi, W.I., Liu, P., Good, W.R., 1992. The effects of ethanol on the transport of lipophilic and polar permeants across hairless mouse skin: methods/validation of a novel approach. Int. J. Pharm. 78, 137–156.

Hashida, M., Okamoto, H., Sezaki, H., 1988. Analysis of drug penetration through skin considering donor concentration decrease. J. Pharmacobio.-Dyn. 11, 636–644.

He, N., Li, S.K., Suhonen, T.M., Warner, K.S., Higuchi, W.I., 2003. Mechanistic study of alkyl azacycloheptanones as skin permeation enhancers by permeation and partition experiments with hairless mouse skin. J. Pharm. Sci. 92, 297–310.

He, N., Warner, K.S., Chantasart, D., Shaker, D., Higuchi, W.I., Li, S.K., 2004. Mechanistic study of chemical permeation enhancers with different polar and lipophilic functional groups. J. Pharm. Sci. 93, 1415–1430.

Kim, Y.H., Ghanem, A.H., Mahmoud, H., Higuchi, W.I., 1992. Short chain alkanols as transport enhancers for lipophilic and polar/ionic permeants in hairless mouse skin mechanism(s) of action. Int. J. Pharm. 80, 17–31.

Liu, P., 1989. The influences of ethanol on simultaneous diffusion and metabolism of estradiol in skin. Ph.D. Thesis, University of Utah, USA.

Mitragotri, S., 2000. In situ determination of partition and diffusion coefficients in the lipid bilayers of stratum corneum. Pharm. Res. 17, 1026–1029.

Okamoto, H., Hashida, M., Sezaki, H., 1988. Structure–activity relationship of 1-alkyl or 1-alkenylazacycloalkanone derivatives as percutaneous penetration enhancers. J. Pharm. Sci. 77, 418–424.

Okamoto, H., Yamashita, F., Saito, K., Hashida, M., 1989. Analysis of drug penetration through the skin by the two-layer skin model. Pharm. Res. 6, 931–937.

Okamoto, H., Hashida, M., Sezaki, H., 1991. Effect of 1-alkyl- or 1-alkenylazacycloalkanone derivatives on the penetration of drugs with different lipophilicities through guinea pig skin. J. Pharm. Sci. 80, 39–45.

Raykar, P.V., Fung, M.C., Anderson, B.D., 1988. The role of protein and lipid domains in the uptake of solutes by human stratum corneum. Pharm. Res. 5, 140–150.

Talreja, P.S., Kleene, N.K., Pickens, W.L., Wang, T.F., Kasting, G.B., 2001. Visualization of the lipid barrier and measurement of lipid pathlength in human stratum corneum. AAPS PharmSci. 3, E13.

Tojo, A., Chiang, C.C., Chien, Y.W., 1987. Drug permeation across the skin: effect of penetrant hydrophilicity. J. Pharm. Sci. 76, 123–126.

Tojo, A., 1988. Concentration profile in plasma after transdermal drug delivery. Int. J. Pharm. 43, 201–205.

Warner, K.S., Li, S.K., Higuchi, W.I., 2001. Influences of alkyl group chain length and polar head group on chemical skin permeation enhancement. J. Pharm. Sci. 90, 1143–1153.

Warner, K.S., Li, S.K., He, N., Suhonen, T.M., Chantasart, D., Bolikal, D., Higuchi, W.I., 2003. Structure–activity relationship for chemical skin permeation enhancers: probing the chemical microenvironment of the site of action. J. Pharm. Sci. 92, 1305–1322.

Xiang, T.X., Anderson, B.D., 1998. Influence of chain ordering on the selectivity of dipalmitoylphosphatidylcholine bilayer membranes for permeant size and shape. Biophys. J. 75, 2658–2671.

Yamashita, F., Yoshioka, T., Koyama, Y., Okamoto, H., Sezaki, H., Hashida, M., 1993. Analysis of skin penetration enhancement based on a two-layer skin diffusion model with polar and nonpolar routes in the stratum corneum: dose-dependent effect of 1-geranylazacycloheptan-2-one on drugs with different lipophilicities. Biol. Pharm. Bull. 16, 690–697.

Yamashita, F., Bando, H., Koyama, Y., Kitagawa, S., Takakura, Y., Hashida, M., 1994. In vivo and in vitro analysis of skin penetration enhancement based on a two-layer diffusion model with polar and nonpolar routes in the stratum corneum. Pharm. Res. 11, 185–191.

Yamashita, F., Koyama, Y., Kitano, M., Takakura, Y., Hashida, M., 1995. Analysis of in vivo skin penetration enhancement by oleic acid based on a two-layer diffusion model with polar and nonpolar routes in the stratum corneum. Int. J. Pharm. 117, 173–179.

Yoneto, K., Ghanem, A.H., Higuchi, W.I., Peck, K.D., Li, S.K., 1995. Mechanistic studies of the 1-alkyl-2-pyrrolidones as skin permeation enhancers. J. Pharm. Sci. 84, 312–317.

Yoneto, K., Li, S.K., Higuchi, W.I., Jiskoot, W., Herron, J.N., 1996. Fluorescent probe studies of the interactions of 1-alkyl-2-pyrrolidones with stratum corneum lipid liposomes. J. Pharm. Sci. 85, 511–517.

Yoneto, K., Li, S.K., Higuchi, W.I., Shimabayashi, S., 1998. Influence of the permeation enhancers 1-alkyl-2-pyrrolidones on permeant partitioning into the stratum corneum. J. Pharm. Sci. 87, 209–214.

Yu, B., Dong, C.-Y., So, P.T.C., Blankschtein, D., Langer, R., 2001. In vitro visualization and quantification of oleic acid induced changes in transdermal transport using two-photon fluorescence microscopy. J. Invest. Dermatol. 117, 16–25.